The American Journal of Pathology, Vol. 170, No. 1, January 2007

DOI: 10.2353/ajpath.2007.060381

Epithelial and Mesenchymal Cell Biology

Asbestos-Induced Peribronchiolar Cell Proliferation and Cytokine Production Are Attenuated in Lungs of Protein Kinase C-δ Knockout Mice

Arti Shukla,* Karen M. Lounsbury,† Trisha F. Barrett,* Joanna Gell,* Mercedes Rincon,‡ Kelly J. Butnor,* Douglas J. Taatjes,* Gerald S. Davis,‡ Pamela Vacek,§ Keiichi I. Nakayama,¶ Keiko Nakayama,¶ Chad Steele,‖ and Brooke T. Mossman*

From the Departments of Pathology, Pharmacology,† Medicine,‡ and Medical Biostatistics,§ University of Vermont, Burlington, Vermont; the Pediatric Pulmonary Division,‖ Children's Hospital of Pittsburgh, Pittsburgh, Pennsylvania; and the Department of Molecular Genetics,¶ Medical Institute of Bioregulation, Kyushu University, Fukuoka, Japan*

The signaling pathways leading to the development of asbestos-associated diseases are poorly understood. Here we used normal and protein kinase C (PKC)-δ knockout (PKCδ$^{-/-}$) mice to demonstrate multiple roles of PKC-δ in the development of cell proliferation and inflammation after inhalation of chrysotile asbestos. At 3 days, asbestos-induced peribronchiolar cell proliferation in wild-type mice was attenuated in PKCδ$^{-/-}$ mice. Cytokine profiles in bronchoalveolar lavage fluids showed increases in interleukin (IL)-1β, IL-4, IL-6, and IL-13 that were decreased in PKCδ$^{-/-}$ mice. At 9 days, microarray and quantitative reverse transcriptase-polymerase chain reaction analysis of lung tissues revealed increased mRNA levels of the profibrotic cytokine, IL-4, in asbestos-exposed wild-type mice but not PKCδ$^{-/-}$ mice. PKCδ$^{-/-}$ mice also exhibited decreased lung infiltration of polymorphonuclear cells, natural killer cells, and macrophages in bronchoalveolar lavage fluid and lung, as well as increased numbers of B lymphocytes and plasma cells. These changes were accompanied by elevated mRNA levels of immunoglobulin chains. These data show that modulation of PKC-δ has multiple effects on peribronchiolar cell proliferation, proinflammatory and profibrotic cytokine expression, and immune cell profiles in lung. These results also implicate targeted interruption of PKC-δ as a potential therapeutic option in asbestos-induced lung diseases. ***(Am J Pathol 2007, 170:140–151; DOI: 10.2353/ajpath.2007.060381)***

Asbestos is a family of crystalline hydrated silicate fibers that cause pulmonary inflammation and fibrosis, as well as cancers of the lung and pleura.[1,2] To date there is no effective therapy for these diseases. After inhalation, asbestos fibers initially interact with bronchiolar and alveolar epithelial cells and alveolar macrophages, which attempt to engulf the fibers. Alveolar macrophages and epithelial cells then become activated, releasing tissue-damaging reactive oxygen species and various cytokines that are thought to initiate alveolitis, fibroblast proliferation, and collagen deposition. Elucidation of the critical cellular and molecular mechanisms initiating and contributing to cell proliferation, inflammation, and fibrogenesis by asbestos fibers is essential to the development of effective therapies for asbestos-induced lung diseases.

The protein kinase C (PKC) family of proteins is comprised of at least 12 isozymes with diverse functions.[3,4] Different isoforms of PKC have been shown to regulate various signaling pathways in different immune cells.[5] PKC-δ is an isoform induced in bronchiolar and alveolar epithelial cells *in vivo* and *in vitro* after exposure to asbestos and after mechanical wounding.[6] Although asbestos activates several isoforms of PKC (ζ, δ, α), PKC-δ uniquely migrates to mitochondria and is causally associated with release of cytochrome *c*, caspase 9 activation, and apoptosis of lung epithelial cells.[7]

Other studies indicate direct and indirect roles of PKC-δ in the regulation of collagen synthesis and fibrosis. PKC-δ plays an important role in modulation of fibrosis via

Supported by the National Institutes of Health (program project grant PO1HL67004) and the National Cancer Institute (grant P30CA22435 to the Vermont Cancer Center DNA Analysis Facility that performed oligonucleotide microarrays and real-time quantitative PCR).

Accepted for publication October 4, 2006.

Address reprint requests to Prof. Brooke T. Mossman, Department of Pathology, College of Medicine, University of Vermont, 89 Beaumont Ave., Burlington, VT 05405. E-mail: brooke.mossman@uvm.edu.

regulation of collagen gene expression in human pulmonary fibroblasts exposed to transforming growth factor-β[8] and in scleroderma fibroblasts.[9] Inhibition of PKC-δ also results in a marked reduction in collagen 1α1 (Col1α1) and collagen 3α1 (Col3α1) mRNA expression and collagen synthesis in lung fibroblasts.[8] Other extracellular matrix proteins such as fibronectin are also regulated by PKC-δ in human dermal fibroblasts.[10] We have recently shown in an asbestos inhalation model of fibrogenesis that transcriptional up-regulation of matrix metalloproteinase (MMP)-12 and MMP-13 occurs via a PKC-δ-dependent pathway.[11]

In addition to direct effects on collagen and MMP regulation, PKC-δ is implicated in regulation of proinflammatory and profibrotic cytokines. For example, PKC-δ and other isoforms of PKC are linked to cell signaling events leading to synthesis of tumor necrosis factor (TNF)-α, interleukin-1β (IL-1β), and interleukin-6 (IL-6) in human monocytes.[12]

Based on these observations, we hypothesized that PKC-δ would modulate parameters of cell proliferation and inflammation linked to the development of fibrogenesis. Using PKC$\delta^{-/-}$ and wild-type (WT) C57BL/6 mice and a well-characterized murine inhalation model of fibrogenesis,[13,14] we demonstrate that PKC-δ plays multiples roles in the pathogenesis of asbestos-induced fibrogenesis. These findings suggest that targeted disruption of the PKC-δ pathway could be a novel strategy for the therapy for asbestos-related diseases in man.

Materials and Methods

Development and Characterization of PKC$\delta^{-/-}$ Mice

A breeding pair of PKC$\delta^{+/-}$ mice originally bred into the C57BL/6 background was a kind gift from Dr. K.I. Nakayama (Department of Molecular Genetics, Medical Institute of Bioregulation, Kyushu University, Fukuoka, Japan).[15] These mice were subsequently maintained and bred into the C57BL/6 background for three to six generations in the UVM facility before use with WT mice in inhalation experiments. Tail DNA was evaluated and typed using the polymerase chain reaction (PCR) and primers for PKC-δ obtained from MWG Biotech. Inc. (High Point, NC). Lung tissue from PKC$\delta^{-/-}$ mice was examined by Western blot analyses using antibodies for PKC-δ and other PKC isoforms (α, ζ, θ) (Santa Cruz Biotechnology, Inc., Santa Cruz, CA) to confirm comparatively that PKC-δ protein was selectively absent in PKC$\delta^{-/-}$ mice and that the expression of other isoforms was normal.

Western Blot Analysis for Different PKC Isoforms

Frozen lung tissue was homogenized in a lysis buffer containing 20 mmol/L Tris, pH 7.6, 1% Triton X-100, 137 mmol/L NaCl, 2 mmol/L ethylenediaminetetraacetic acid, 1 mmol/L Na_3VO_4, 1 mmol/L dithiothreitol, 1 mmol/L phenylmethyl sulfonyl fluoride, 10 μg/ml leupeptin, and 10 μg/ml aprotinin before incubation on ice for 30 minutes. Cells were then sonicated and centrifuged at 14,000 rpm for 15 minutes at 4°C. Supernatants were collected, and protein concentrations were determined with the Bradford assay (Bio-Rad, Hercules, CA). Western blots with 40-μg lysates were performed as described earlier[11] using antibodies specific for different isoforms of PKC-δ (Santa Cruz Biotechnology) at 1:500 (PKC-δ, -ζ, -α, -θ) dilution. Antibody binding was visualized by enhanced chemiluminescence (Amersham Pharmacia Biotech, Piscataway, NJ) according to the manufacturer's protocol.

Inhalation Experiments

Animal experiments were conducted in accordance with the National Institutes of Health Guide for the Care and Use of Laboratory Animals (1985), and protocols approved by the University of Vermont Institutional Animal Care and Use Committee. In duplicate experiments, six mice (8 to 12 weeks of age) were exposed to ambient air or the National Institute of Environmental Health Sciences reference sample of chrysotile asbestos[16] (7 mg/m^3 air, 6 hours/day, 5 days/week) for 3, 9, or 40 days as described previously.[13,14]

Bronchoalveolar Lavage Fluid (BALF) and Assays

After asbestos exposure for 3, 9, or 40 days, five to eight mice at each time point from each of four exposure groups (sham WT, asbestos WT, sham PKC$\delta^{-/-}$, asbestos PKC$\delta^{-/-}$) received a lethal dose of pentobarbital (Abbott Laboratories, Abbot Park, IL). Chest cavities were opened, and lungs were cannulated via the trachea with polyethylene tubing. Lungs were then lavaged *in situ* with sterile Ca^{2+}- and Mg^{2+}-free phosphate-buffered saline at a volume of 1 ml. The volume of retrieved phosphate-buffered saline (PBS) in BALF was also recorded. BALFs were centrifuged at 1000 rpm at 4°C to obtain a cell pellet for total and differential cell counts. Cytocentrifuge preparations were stained with Giemsa and May-Grunwald stains, coverslipped, and 500 cells counted on each of two slides.

Bio-Plex Analysis of Bronchoalveolar Lavage Cytokine and Chemokine Concentrations

To quantify cytokine and chemokine levels in BALF supernatant, a multiplex suspension protein array was performed using the Bio-Plex protein array system and a Mouse Cytokine 22-plex panel (Bio-Rad) as described previously.[14] This method of analysis is based on Luminex technology and simultaneously measures IL-1α, IL-1β, IL-2, IL-4, IL-5, IL-6, IL-9, IL-10, IL-12(p40), IL-12(p70), IL-13, IL-17, TNF-α, regulated on activation normal T cell expressed and secreted (RANTES), MIP-1α, macrophage inflammatory protein (MIP)-1β, mono-

cyte chemoattractant protein (MCP)-1, keratinocyte-derived chemokine (KC), granulocyte cell-stimulating factor (G-CSF), granulocyte macrophage-colony-stimulating factor (GM-CSF), interferon (IFN)-γ, and eotaxin protein. Concentrations of each cytokine and chemokine were determined using Bio-Plex Manager version 3.0 software.

Histopathology

After collection of BALF, lungs were inflated with a 1:1 mixture of Optimum Cutting Temperature (OCT; Tissue-Tek, Torrance, CA) and PBS. Lung sections (5 μm in thickness) were used for immunohistochemistry or stained with hematoxylin and eosin (H&E), the Masson's trichrome technique for detection of collagen, or methyl green-pyronin to identify plasma cells[17] (Sigma-Aldrich, St. Louis, MO). All lung sections were scored for inflammation (H&E) and collagen deposition (extent and severity of fibrosis) (Masson's trichrome) by a board-certified pathologist (K.J.B.) using a blinded coding and scoring system.[18] More than five mouse lungs were examined in each group at each time point.

Immunoperoxidase Technique for Ki-67 and CD45

To measure cell proliferation, sections were evaluated using an antibody to Ki-67, a marker of cycling cells,[19] as described previously.[20] Ki-67-positive cells were quantitated in three compartments: distal bronchiolar epithelium/alveolar duct epithelium, the peribronchiolar compartment of these same bronchioles, and the lung interstitium excluding vessels and bronchioles. Distal bronchioles evaluated were restricted to those with less than an 800-μm perimeter when viewed at $\times$400 magnification. Ki-67-positive cells in all compartments presented with distinct brown versus purple nuclei, and the total number of Ki-67-positive and -negative nuclei from all bronchioles on a lung section and their peribronchiolar region were quantitated to obtain an average of the percentage of positively stained cells per animal. For the interstitial compartment, an image of the interstitium of the lung was viewed at $\times$400 with a 5 $\times$ 4 grid superimposed. For each image, the percentage of Ki-67-positive cells in five boxes, excluding blood vessels and bronchioles, was determined to achieve an average (means $\pm$ SEM) per animal. To detect lymphocyte staining in lungs, sections were probed for CD45R/B220 (1:100 dilution; Pharmingen, Franklin Lakes, NJ) and processed as described above for Ki-67.

Ki-67/CD45 Co-Localization Using Dual Immunofluorescence

Slides were deparaffinized followed by rehydration in a graded ethanol series. After rinsing with H_2O, slides were placed in antigen retrieval solution (DakoCytomation, Carpinteria, CA). After antigen retrieval, slides were permeabilized in 0.1% Triton X in PBS and were blocked in 10% normal goat serum (Jackson Laboratories, Bar Harbor, ME). Ki-67 antibody (rat monoclonal 1:25; DakoCytomation) was applied to each slide and incubated overnight at 4°C. The following day slides were washed and incubated in secondary antibody (1:400 goat anti-rat Alexa Fluor 568; Molecular Probes, Eugene, OR). Next, slides were fixed in 3% paraformaldehyde for 30 minutes followed by three washes in PBS. Antigen retrieval was repeated before the addition of the CD45 primary antibody (rat monoclonal 1:500; Caltag, Burlingame, CA) overnight at 4°C. After two washes in PBS, slides were incubated with secondary antibody (1:400 goat anti-rat Alexa Fluor 647; Molecular Probes) for 1 hour at room temperature. Slides were washed, coverslipped, and visualized using a MRC1024 ES confocal laser-scanning microscope (Bio-Rad).

Flow Cytometry of Lung, Spleen, and BALF Cells

Isolation of Lung and Spleen Cells

Lung mononuclear cells were isolated by collagenase enzyme digestion and gentle mechanical disruption.[21] Spleen cell suspensions were prepared by pressing the spleen between frosted ends of glass microscope slides to disrupt the tissue by gentle shearing pressure and then rinsing with Dulbecco's modified Eagle's medium and 5% fetal bovine serum (FBS).[21] Cells were counted using a hemocytometer before analysis by flow cytometry after antibody staining.

Surface Antigen Staining

Cell pellets in each tube were resuspended in 100 μl of PBS-1% FBS-FcBlock (1:200) to block nonspecific adherence of staining antibodies, incubated for 10 minutes at 4°C, and centrifuged, and the supernatant was discarded. The pellet then was suspended in 100 μl of PBS/FBS containing a mixture of fluorochrome-labeled surface marker antibodies. The antibodies used are summarized in Table 1. Cells were stained for 30 minutes in the dark at 4°C and then washed 2$\times$ in 500 μl of PBS/FBS. If secondary antibody was required, the above procedure was repeated for a second incubation followed by washes. Finally, cells were resuspended in 100 μl of 1% paraformaldehyde and 300 μl of PBS/FBS for flow analysis.

Flow Cytometry

Cell samples after staining were examined in a dual-laser four-color Coulter EPICS Elite cytofluorograph using Coulter Elite analysis software (Coulter, Hialeah, FL), and evaluating at least 40,000 cells per sample. Each sample population was classified for cell size (forward scatter) and complexity (side scatter), and a gate of interest was drawn around the viable small mononuclear cell population, excluding debris and erythrocytes. Each cell within this gate was categorized for fluorescence intensity in the color channel relevant for each of the surface antigen or

Table 1. Fluorescence Antibodies Used for Flow Cytometry

Target antigen	Target cell type	Fluorochrome	Reagent source
CD4	Helper/induced T cells	Alexa 647	Life Technologies (Philadelphia, PA)
CD8	Suppressed/cytolytic T cells	Texas Red 615	Caltag (Burlingame, CA)
γ/δ TCR	T-cell subset	Biotin/strep 647	Pharmingen (San Jose, CA)
β TCR	T-cell subset	Cytochrome	Caltag
DX5 (NK cells)	NK cells	PE	Pharmingen
NK1.1	NK cells	FITC	Pharmingen
B220	B lymphocytes	PE	Caltag
MAC1	Macrophages	FITC	Pharmingen

cytokine antibody fluorochromes. The results were expressed as the percentage of cells within the size/complexity gate of interest that stained positively for each marker after subtracting the percentage of positive cells in the isotype control.

Microarray Analysis

At 9 days, total RNA was isolated from lung tissues of mice (n = 3 per group) using Trizol reagent (Invitrogen, Life Technologies, Carlsbad, CA),[22] and after purification samples were submitted to the Vermont Cancer Center Microarray Facility for target preparation using standard Affymetrix protocols.[14] In brief, 3 μg of total RNA from each sample was reverse-transcribed using oligo-dT primer coupled to a T7 RNA polymerase binding sequence. After double-stranded cDNA preparation, biotinylated-cRNA was synthesized using T7 polymerase, and hybridized to Affymetrix murine genome U74Av2 (Affymetrix Inc., Santa Clara, CA) oligonucleotide arrays for 16 hours. The arrays were first incubated with phycoerythrin-conjugated streptavidin, followed by sequential incubations with biotin-coupled polyclonal anti-streptavidin antibody and streptavidin-phycoerythrin as an amplification step. After washing and laser scanning (Hewlett-Packard GeneArray Scanner; Agilent Technologies, Inc., Santa Clara, CA), data were collected and analyzed using GeneSifter software (GeneSifter VizX Labs, Seattle, WA). Data were log-transformed for analyses.

TaqMan Quantitative Reverse Transcriptase-Polymerase Chain Reaction (QRT-PCR)

Gene expression data from microarray analysis was confirmed by QRT-PCR using primers and probes purchased from Applied Biosystems (Foster City, CA) as described previously.[14] The Perkin-Elmer AB1 7700 Prism sequence detection system (Applied Biosystems) was used to determine relative levels of expression of different immunoglobulins and IL-4. All values were normalized to the expression of *hprt*.

Statistical Analyses

Results were evaluated by one-way analysis of variance with the Student-Newman-Keul's procedure for adjustment of multiple pairwise comparisons between treatment groups. For cytokines, statistical analyses were performed using the nonparametric Kruskul-Wallis test because analysis of variance was inappropriate because of differing variability in the treatment groups. Differences of $P \leq 0.05$ were considered statistically significant. Data for severity and extent of fibrosis (n = 8 to 13 mice/group/per experiment) were analyzed by analysis of variance using a randomized block design to control for differences between experiments.

Results

We present data on cell proliferation at 3, 9, and 40 days and inflammation and cytokines in BALF at 3 and 9 days (because all cytokine levels were diminished and showed no statistical changes at 40 days).

PKCδ$^{-/-}$ Mice Exhibit Selective Depletion of PKC-δ in Lung Tissue

Lung tissues from PKCδ$^{-/-}$ and WT mice were evaluated by Western blot analyses for four different PKC isoforms present in lung or murine epithelial cells (Figure 1A).[6,7] These results confirmed that PKCδ$^{-/-}$ mice lacked only PKC-δ protein, whereas other isoforms of PKCs (ζ, θ, α) were present. These data indicate that no compensation for loss of PKC-δ protein occurs by other isoforms of PKC in PKCδ$^{-/-}$ mice.

PKCδ$^{-/-}$ Mice Exhibit Less Acute Peribronchiolar Cell Proliferation than Asbestos-Exposed WT Mice

We have shown recently that the peak time point of epithelial cell proliferation, as measured by incorporation of Ki-67, occurs after 3 days of asbestos inhalation by C57BL/6 WT mice.[14] In studies here, we also measured cell proliferation in various lung compartments after 3, 9, and 40 days of asbestos inhalation to determine whether they were altered by PKC-δ status. Bronchiolar epithelial cell proliferation was increased ($P \leq 0.05$) in both PKCδ$^{-/-}$ and WT mice at all time points (Figure 1B). However, peribronchiolar cell proliferation peaked at 3 days in asbestos-exposed WT mice but was significantly inhibited ($P \leq 0.05$) in asbestos-exposed PKCδ$^{-/-}$ mice at this time point (Figure 1C). Numbers of Ki-67-positive cells in the interstitial com-

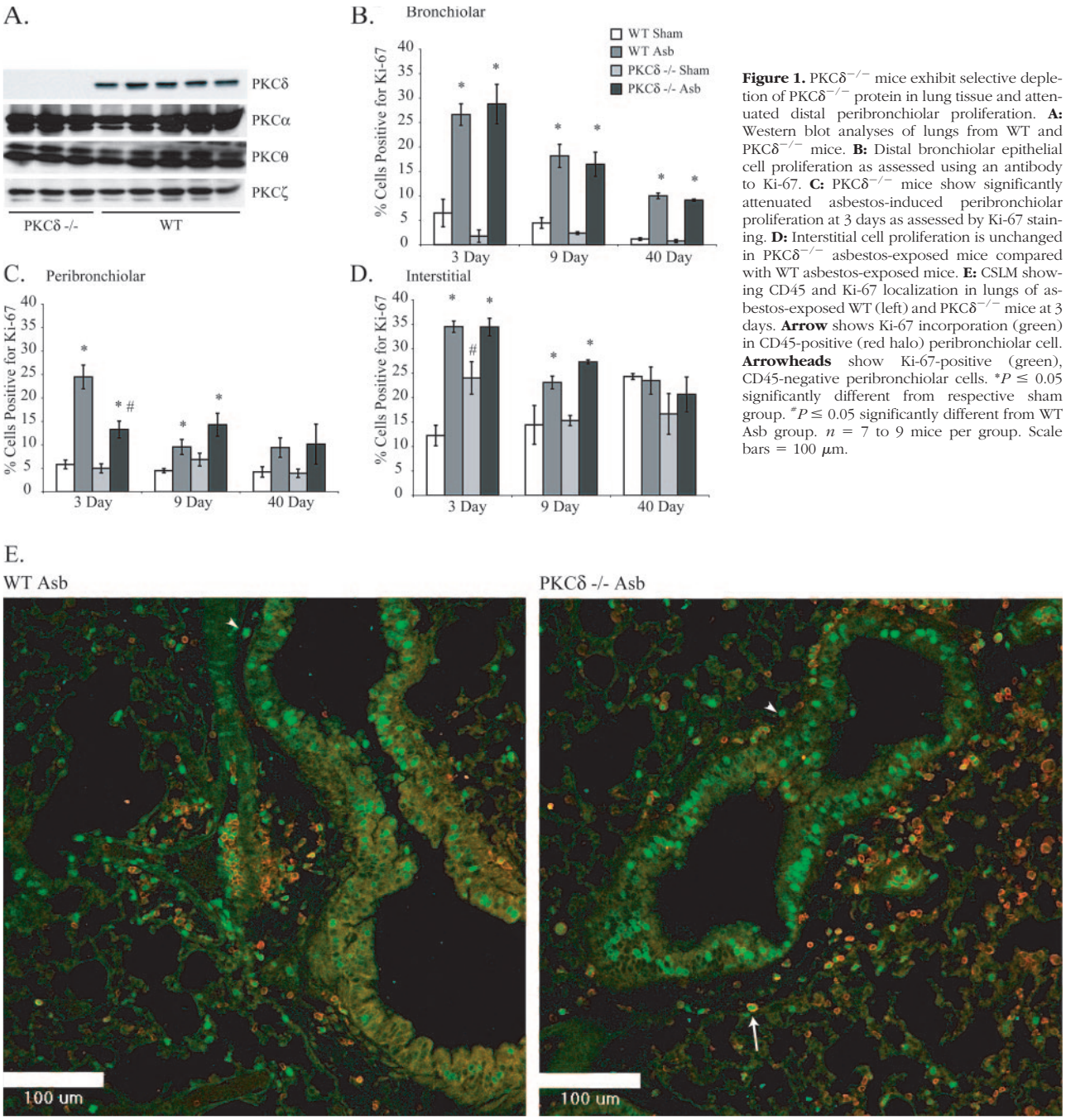

Figure 1. PKCδ$^{-/-}$ mice exhibit selective depletion of PKCδ$^{-/-}$ protein in lung tissue and attenuated distal peribronchiolar proliferation. **A:** Western blot analyses of lungs from WT and PKCδ$^{-/-}$ mice. **B:** Distal bronchiolar epithelial cell proliferation as assessed using an antibody to Ki-67. **C:** PKCδ$^{-/-}$ mice show significantly attenuated asbestos-induced peribronchiolar proliferation at 3 days as assessed by Ki-67 staining. **D:** Interstitial cell proliferation is unchanged in PKCδ$^{-/-}$ asbestos-exposed mice compared with WT asbestos-exposed mice. **E:** CSLM showing CD45 and Ki-67 localization in lungs of asbestos-exposed WT (left) and PKCδ$^{-/-}$ mice at 3 days. **Arrow** shows Ki-67 incorporation (green) in CD45-positive (red halo) peribronchiolar cell. **Arrowheads** show Ki-67-positive (green), CD45-negative peribronchiolar cells. $^{*}P \leq 0.05$ significantly different from respective sham group. $^{\#}P \leq 0.05$ significantly different from WT Asb group. n = 7 to 9 mice per group. Scale bars = 100 μm.

partment of the lung peaked in both groups of asbestos-exposed mice at 3 days and remained elevated ($P \leq 0.05$) at 9 days (Figure 1D). To determine whether Ki-67-positive peribronchiolar cells were leukocytes (CD45^{+}) or fibroblasts (CD45^{-}), dual immunofluorescence approaches were used. These studies revealed that Ki-67 was incorporated by both CD45-positive leukocytes (green nuclei with red halo) as well as CD45-negative cells, presumably fibroblasts (green label alone) (Figure 1E). These data show the involvement of PKC-δ in asbestos-induced peribronchiolar proliferation in different cell types.

PKCδ$^{-/-}$ Mice Show Different BALF Cytokine Profiles in Response to Asbestos Exposure

Cytokine analyses on BALF at 3 and 9 days showed low and comparable levels of cytokines in sham WT and PKCδ$^{-/-}$ mice. In asbestos-exposed WT mice at 3 days, significantly increased levels of many cytokines [IL-1α, IL-1β, IL-4, IL-5, IL-6, IL-10, IL-12(p40), IL-13, RANTES, MIP-1α, MIP-1β, MCP-1, KC, G-CSF, and GM-CSF] occurred. Many of these [IL-4, IL-5, IL-10, IL-12(p40), IL-12 (p70), IL-13, RANTES, MIP-1α, MCP-1, KC, and GM-CSF] were significantly attenuated in asbestos-exposed

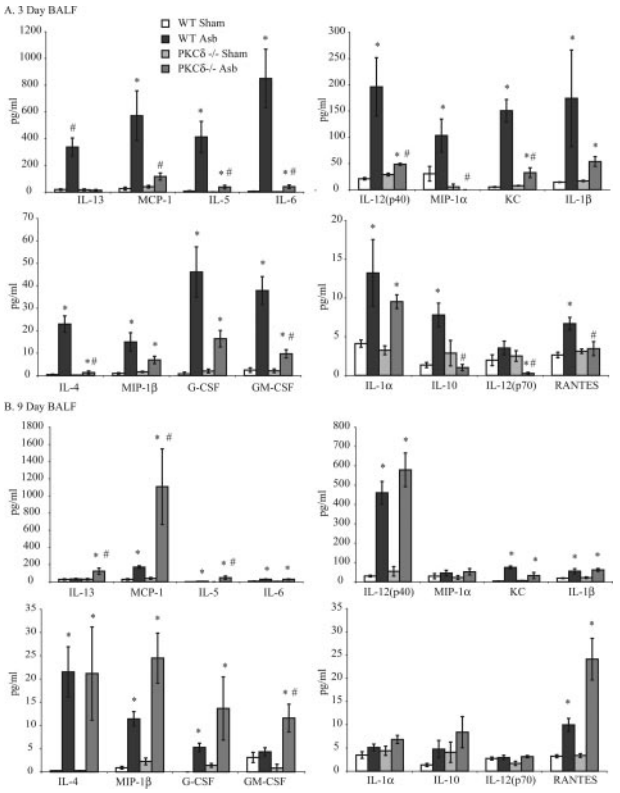

Figure 2. Asbestos-induced increases in BALF cytokine levels were attenuated in PKC$\delta^{-/-}$ mice at 3 days. Bioplex assays were performed on the supernatants of BALF samples collected at 3 (**A**) and 9 (**B**) days after asbestos inhalation as described in the Materials and Methods section. $^{*}P \leq 0.05$, significantly different from respective sham group; $^{\#}P \leq 0.05$, significantly different from WT Asb group.

PKC$\delta^{-/-}$ mice (Figure 2A). After 9 days of asbestos exposure, levels of IL-13, MIP-1α, GM-CSF, IL-1α, and IL-10 were similar in sham- and asbestos-exposed WT mice whereas other cytokines, MCP-1, IL-12(p40), KC, IL-1β, IL-4, MIP-1β, G-CSF, and RANTES remained elevated (Figure 2B). Levels of IL-13, MCP-1, IL-5, and GM-CSF were elevated ($P \leq 0.05$) in asbestos-exposed PKC$\delta^{-/-}$ versus WT mice. Levels of TNF-α were highly variable between animals, and there was no change in IFN-γ, IL-17, or eotaxin levels between groups at any time (data not shown). Trends in increased expression of IL-4, a profibrotic cytokine that was increased in BALF from asbestos-exposed WT mice selectively at 3 days and in asbestos-inhaling PKC$\delta^{-/-}$ mice at 9 days (Figure 2), were confirmed in lungs of mice by both microarray (Figure 3A) and TaqMan analyses (Figure 3B). Data presented here show that PKC-δ plays an important role in regulation of many cytokines, which could eventually be responsible for altered lung pathology of lung in asbestos-exposed PKC$\delta^{-/-}$ mice.

PKC$\delta^{-/-}$ Mice Show Altered Immune Cell Profiles Compared with WT Mice after Asbestos Inhalation

The initial characterization of PKC$\delta^{-/-}$ mice showed that these mice exhibited increased proliferation of B cells in the spleen and evidence of autoimmunity.[15] To determine possible alterations in the lung and systemic inflammation that might explain their resistance to asbestos-induced fibrogenesis, we characterized a number of inflammatory parameters in lung, spleen, and BALF.

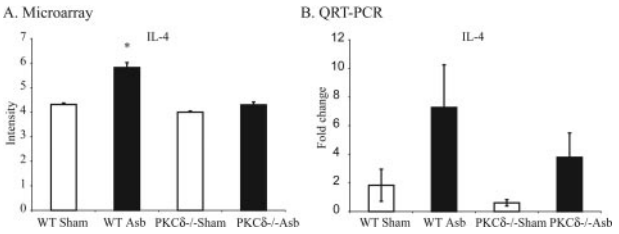

Figure 3. Asbestos-exposed PKC$\delta^{-/-}$ mice exhibit attenuated IL-4 mRNA levels in lungs at 9 days. RNA obtained from lungs of four groups of mice after asbestos inhalation for 9 days was subjected to microarray analysis and results were subsequently validated by real-time quantitative PCR. **A:** Results from microarray analysis. Data were log-transformed for analysis using the GeneSifter program. **B:** Validation of results by real-time quantitative PCR (TaqMan). $^{*}P \leq 0.05$, significantly different from WT sham group.

WT mice exposed to asbestos exhibited substantial elevations in the percentages of polymorphonuclear cells (PMNs) in BALF at 3 (30%) and 9 (80%) days (Figure 4A). In contrast, asbestos-exposed PKC$\delta^{-/-}$ mice showed no increases in PMNs or lymphocytes at 3 days and modestly increased fractions at 9 days. Both sham control groups had few PMNs or lymphocytes. At 9 days, BALF from asbestos-exposed PKC$\delta^{-/-}$ mice revealed increases in lymphocytes ($P \leq 0.05$) and alveolar macrophages in contrast to the predominantly PMN influx (>80%) observed in WT animals (Figure 4A). In addition, a significantly increased proportion ($P \leq 0.05$) of other cells that did not conform to characteristics of lymphocytes, alveolar macrophages, or PMNs were observed in asbestos-exposed PKC$\delta^{-/-}$ mice, and they required further characterization (see below).

Histological analysis of lung sections from asbestos-exposed animals at 9 days showed moderate cellular inflammation and sporadic increases in alveolar-ductal cellularity (Figure 4B). Increased lung infiltration of macrophages, PMNs, and lymphocytes were observed in asbestos-exposed WT and PKC$\delta^{-/-}$ animals; however, lymphocyte infiltration increased whereas PMN numbers were lower in lungs of PKC$\delta^{-/-}$ mice compared with WT mice (Table 2).

To identify the proportion of cell types present in lung, BALF, and spleen, flow cytometric analysis was performed at 9 days using a set of cell type-specific antibodies (Table 1). As shown in Figure 5A, the percentage of macrophages was significantly attenuated ($P \leq 0.05$) in sham PKC$\delta^{-/-}$ mice compared with sham WT mice. Data using two antibodies detecting natural killer (NK) cells (DX5 also stains macrophages and mesenchymal cells, whereas NK1.1 labels some NK as well as NKT cells) also indicated decreased proportions in PKC$\delta^{-/-}$ versus WT mice after inhalation of asbestos. CD4-positive T cells were increased in lungs of asbestos-exposed WT and PKC$\delta^{-/-}$ mice (Figure 5A). In BALF preparations, numbers of NK cells were attenuated in both sham- and asbestos-exposed PKC$\delta^{-/-}$ mice (Figure 5B), as was observed in lung tissue (Figure 5A). Increased percent-

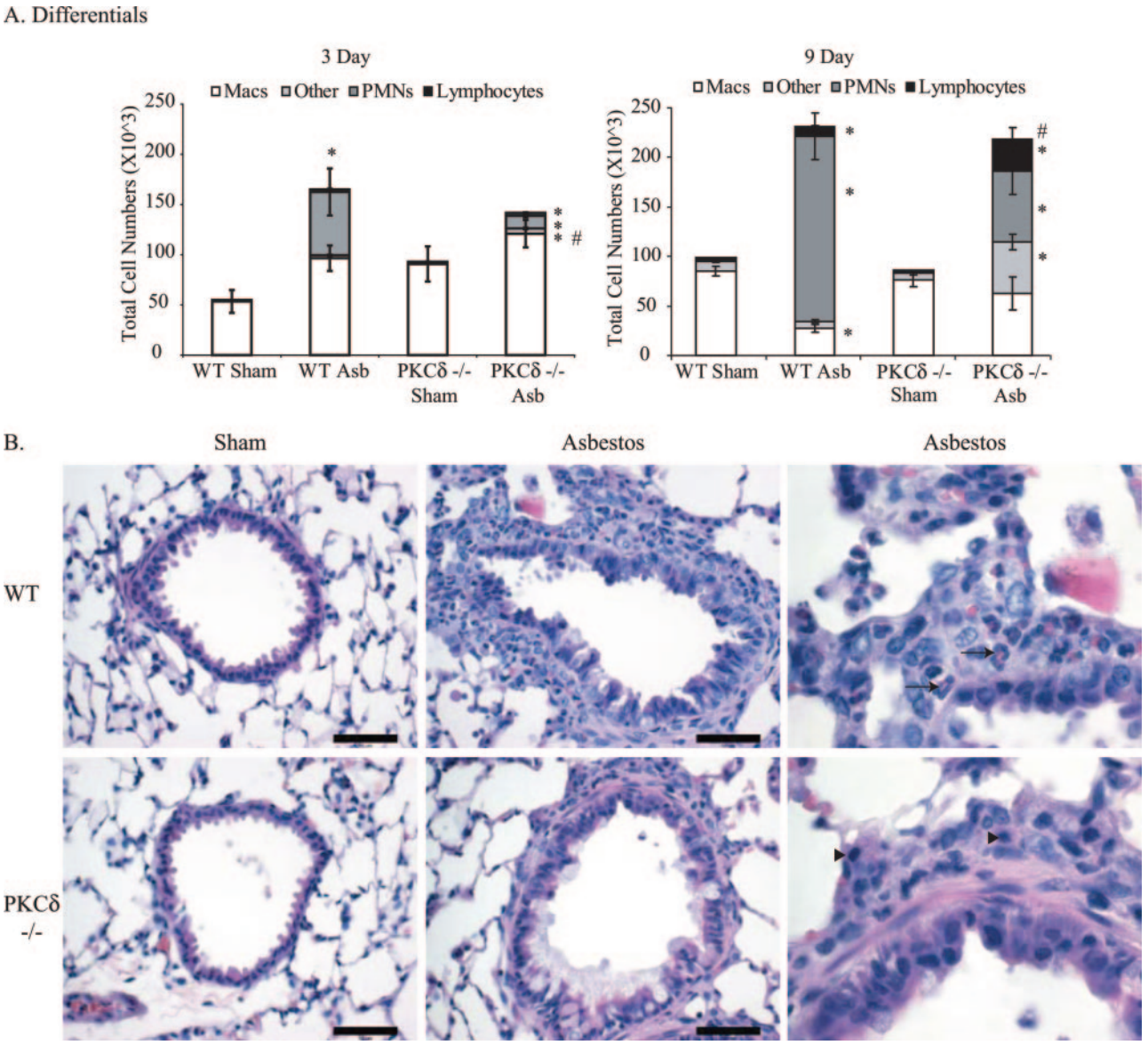

Figure 4. PKC$\delta^{-/-}$ mice show altered inflammatory profiles in BALF after asbestos inhalation. **A:** Differential cell counts on BALF at 3 and 9 days. $^{*}P \leq 0.05$, significantly different from respective sham group; $^{\#}P \leq 0.05$, significantly different from WT Asb group. **B:** Histopathology of distal bronchioles at 9 days after H&E staining. In comparison to sham mice (left), asbestos-exposed mice show pronounced peribronchiolar inflammation that is characterized by predominantly neutrophil infiltration (**arrows**) in WT mice and lymphocytes in PKC$\delta^{-/-}$ mice (**arrowheads**). Scale bars = 50 μm.

ages of B and T cells also were observed in asbestos-exposed WT and PKC$\delta^{-/-}$ mice (Figure 5B). In spleen, both macrophages and NK cells were decreased in PKC$\delta^{-/-}$ sham- and asbestos-exposed animals, but no differences in numbers of CD4- and CD8-positive T cells were observed between groups (Figure 5C). Elevations ($P \leq 0.05$) in B lymphocytes were observed in asbestos-exposed PKC$\delta^{-/-}$ mice. PKC$\delta^{-/-}$ mice also showed increased spleen weight (Figure 5D) as reported previously.[15] For detailed characterization of B cells, CD19 and

Table 2. Immune Cell Profiles at 9 Days in Lung Tissue

	n	Macrophages	PMNs	Lymphocytes
WT sham	13	1.583 ± 0.144*	1.077 ± 0.077	1.154 ± 0.104
WT asbestos	13	3.231 ± 0.166†	3.308 ± 0.175†	1.846 ± 0.191†
PKC-$\delta^{-/-}$ sham	9	1.778 ± 0.222	1.000 ± 0.000	1.222 ± 0.222
PKC-$\delta^{-/-}$ asbestos	9	3.444 ± 0.242†	2.889 ± 0.200†‡	3.222 ± 0.278†‡

*Score of 1 to 4 based on extent of infiltration.
$^{\dagger}P \leq 0.05$ compared with respective sham.
$^{\ddagger}P \leq 0.05$ compared with WT asbestos-exposed group.

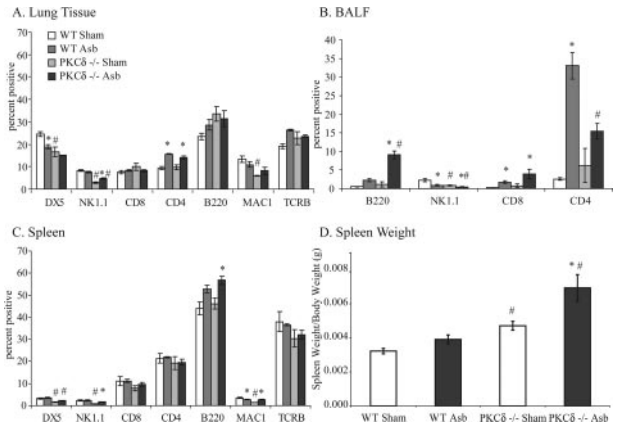

Figure 5. Flow cytometric analyses reveals increased B cells and decreased NK cells in lung, BALF, and spleen of 9-day asbestos-exposed PKCδ$^{-/-}$ mice. Both WT and PKCδ$^{-/-}$ mice were exposed to asbestos for 9 days, and lung, spleen, and BALF cells were prepared for flow cytometric analyses as described in the Materials and Methods section **A:** Flow analyses on lung homogenates. **B:** Flow analyses on BALF cells. **C:** Flow analyses on spleen homogenates. **D:** PKCδ$^{-/-}$ mice showed increased spleen weight as compared with WT mice. $^{*}P \leq 0.05$, significantly different from respective sham group; $^{\#}P \leq 0.05$, significantly different from WT with the same treatment.

IgM antibodies along with B220 were also used (data not shown).

Both sham- and asbestos-exposed PKCδ$^{-/-}$ mice showed unusual patches of cells resembling lymphocytes around blood vessels and bronchioles. Further immunohistochemical characterization of these lymphocytic lesions in lung sections of PKCδ$^{-/-}$ sham- and asbestos-exposed mice showed that CD45R/B220-positive cells were absent from sham WT mice (Figure 6A), were observed occasionally in asbestos-exposed WT mice (Figure 6A) and comprised the majority of cells in lymphocytic patches of both sham- and asbestos-exposed PKCδ$^{-/-}$ mice (Figure 6A). Methyl pyronin-green staining of both lung (Figure 6B) and spleen sections (data not shown) showed the presence of plasma cells in PKCδ$^{-/-}$ sham- and asbestos-exposed mice.

Microarray Analyses Show Increased Expression of Immunoglobulin Chains in PKCδ$^{-/-}$ Murine Lung Tissue

Microarray analyses performed on the lungs of mice at 9 days showed increased mRNA levels for several different immunoglobulin chains in PKCδ$^{-/-}$ sham- and asbestos-exposed mice when compared with WT groups (Figure 7) (data were log transformed for analyses). Microarray data for increases in expression of IgG heavy chain, Ig joining chain, Ig active λ chain, and Ig heavy chain were validated by QRT-PCR (TaqMan) (Figure 8). Increased mRNA levels of different fractions of immunoglobulin chains are additional evidence in support of the presence of plasma cells in lungs of PKCδ$^{-/-}$ mice.

Discussion

Idiopathic pulmonary fibrosis and pulmonary fibrosis associated with the inhalation of asbestos fibers and other

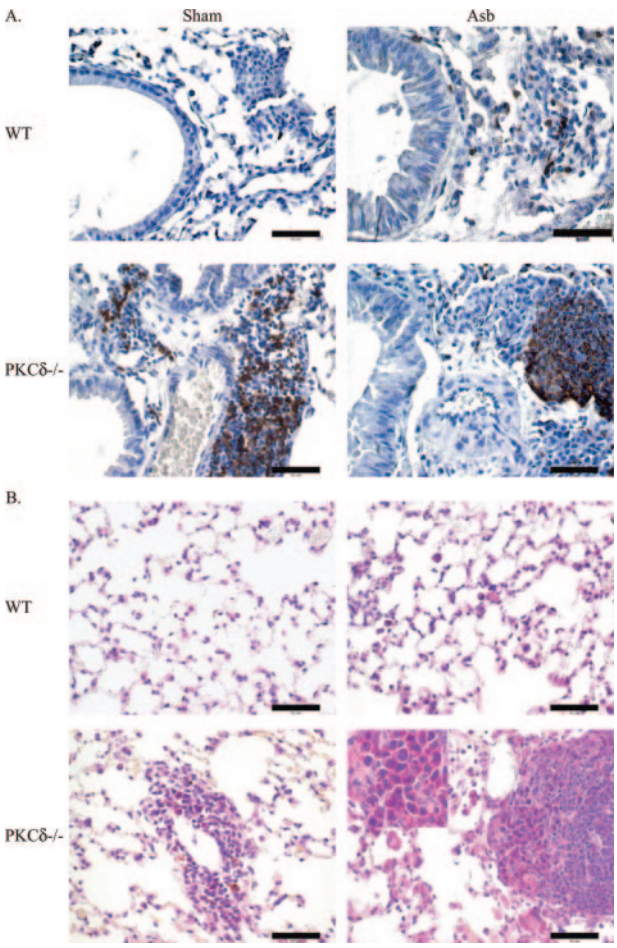

Figure 6. Lungs of PKCδ$^{-/-}$ mice show characteristic patches of cells comprised of lymphocytes and plasma cells. Formalin-fixed lungs from both WT and PKCδ$^{-/-}$ mice with or without asbestos exposure for 9 days were stained for B lymphocytes or plasma cells as described in the Materials and Methods section **A:** Immunoperoxidase staining with a B220/CD45R antibody. **B:** Lung sections stained with methyl pyronin-green to identify plasma cells. Scale bars = 50 μm. Original magnification, ×100 inset.

fibrogenic minerals such as silica are devastating diseases.[23] Current therapeutic approaches, such as corticosteroids and immunosuppressants, are ineffective. Understanding the mechanisms of pathogenesis of fibrotic lung diseases and their inhibition allows the development of new therapeutic paradigms. Data here reveal multiple effects of PKC-δ deficiency on asbestos-induced cell proliferation, cytokine elaboration, and recruitment of inflammatory cell types to lung in a murine model of fibrogenesis.

Although focal peribronchiolar fibrosis and fibrosis in adjacent alveolar ducts/peribronchiolar tiers of alveoli were observed histologically in both asbestos-exposed WT and PKCδ$^{-/-}$ mice at 40 days, and the extent of affected bronchioles was less in PKCδ$^{-/-}$ mice (data not shown), biochemical verification of fibrosis by chrysotile asbestos in mice may require more extended periods of inhalation. For example, in inhalation studies using rats, a more sensitive species to the development of lung injury and fibrosis by particulates, elevations in fibrosis, a biochemical marker of collagen synthesis were observed after inhalation of crocidolite, but not chrysotile asbestos

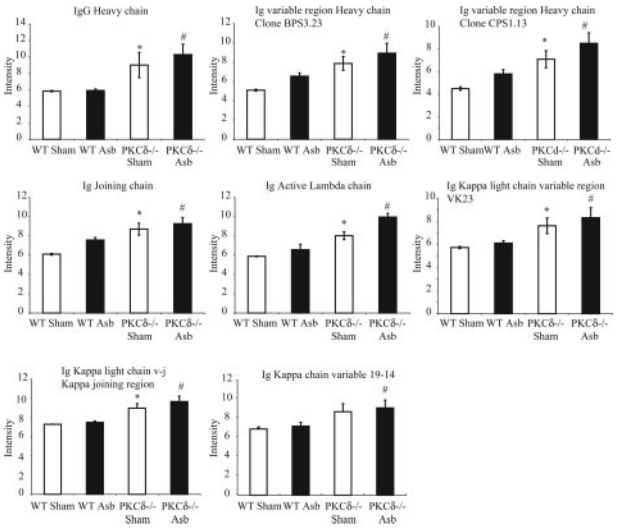

Figure 7. PKC$\delta^{-/-}$ mice show increased mRNA levels of immunoglobulins in lung. Microarray analysis was performed on RNA obtained from lungs of 9-day sham/asbestos-exposed WT and PKC$\delta^{-/-}$ mice. The GeneSifter program was used to analyze the data. The data were log transformed for analyses. $^{*}P \leq 0.05$, significantly different from WT sham group; $^{\#}P \leq 0.05$, significantly different from WT Asb group.

at similar airborne concentrations for 20 days.[24] These observations are in agreement with studies in humans suggesting that chrysotile asbestos is less potent than crocidolite asbestos in inducing asbestos-associated diseases.[1,2]

Chrysotile asbestos-induced fibrogenesis in rodents occurs proximally to initial sites of deposition of fibers in the distal bronchioles and alveolar duct region.[13,14] In WT mice, acute increases in distal bronchiolar epithelial cell, peribronchiolar and interstitial cell proliferation occurred at 3 days after initial exposure to fibers and decreased throughout time (Figure 1). In line with many observations that PKC-δ plays complex roles in cell proliferation and survival,[25] PKC$\delta^{-/-}$ mice showed selective inhibition of peribronchiolar cell proliferation by asbestos. Many Ki-67-labeled peribronchiolar cells were spindle-shaped in morphology and CD45-negative, indicating that they were of mesenchymal origin. The fact that proliferation of these cells was inhibited in PKC$\delta^{-/-}$ mice that developed less fibrosis suggests that targeted interruption of PKC-δ may curtail early replication of cells that may contribute to formation of fibrotic lesions.

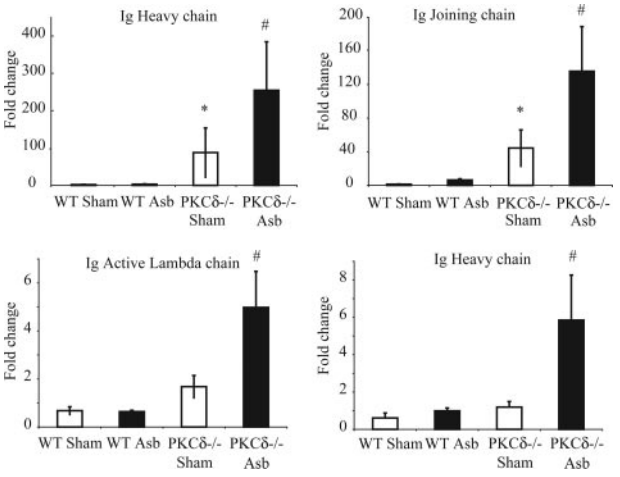

Figure 8. Real-time quantitative PCR validated the changes in immunoglobulins observed with microarray. RNA obtained from lungs of different groups of mice was evaluated using specific primers and probes as described in the Materials and Methods section. $^{*}P \leq 0.05$, significantly different from WT sham group; $^{\#}P \leq 0.05$, significantly different from WT Asb group.

Consistent with the documented roles of individual PKCs in development and modulation of immune responses in other organs,[5] different immune cell profiles were observed in BALF and lungs from PKC$\delta^{-/-}$ and WT mice. Most notably, increases in plasma cells and decreases in numbers of PMNs were observed in PKC$\delta^{-/-}$ mice in contrast to asbestos-exposed WT mice. As suggested here and in a model of reperfusion injury after transient ischemia,[26] PKC-δ deficiency is associated with reduced infiltration of PMNs into damaged lung tissue and impaired neutrophil adhesion, migration, and function.[26] Asbestos-exposed PKC$\delta^{-/-}$ mice also showed significantly reduced levels of KC, a neutrophil chemoattractant,[27] a phenomenon that might explain the lower numbers of PMNs seen in the BALF of these animals. Our recent work, using myeloperoxidase knockout mice, suggests that PMN-associated myeloperoxidase activity is critical to the development of early lung injury and inflammation by asbestos.[20] Moreover, *in vitro* studies show that co-culture with PMNs exacerbates asbestos-induced cell injury to alveolar epithelial cells by oxidant-dependent mechanisms.[28]

Initial characterization of PKC$\delta^{-/-}$ mice showed splenomegaly, reflecting increased numbers of peripheral B cells, although no noteworthy abnormalities were observed in T cells.[15] Histological examination of the kidneys of PKC$\delta^{-/-}$ mice revealed evidence of glomerulonephritis, and immunohistochemical staining revealed deposition of IgG and the complement component C3 in the mesangial region and along capillary walls. Furthermore, perivascular infiltration of leukocytes was detected in the kidney, liver, lungs, and salivary glands of PKC$\delta^{-/-}$ mice. The infiltrating leukocytes were comprised mostly of B lymphocytes with smaller numbers of T lymphocytes also present. These observations suggest that B-cell tolerance is abrogated in PKC$\delta^{-/-}$ mice because of loss of the anti-proliferative activity of PKC-δ.[15] Although NK cells attenuate bleomycin-induced pulmonary fibrosis in mice by producing IFN-γ,[29] numbers of NK cells decreased in lung tissue and BALF from asbestos-exposed WT and PKC$\delta^{-/-}$ mice, suggesting that they are not critical in the development or control of asbestosis. However, the fact that numbers of $CD4^{+}$ cells were diminished in asbestos-exposed PKC$\delta^{-/-}$ mice may explain in part the inhibition of fibrosis in these animals.

A unique feature of the lungs of both sham- and asbestos-exposed PKC$\delta^{-/-}$ mice were peribronchiolar aggregates of plasma cells with lesser numbers of interspersed lymphocytes (Figure 6). The cellular composition of these aggregates was confirmed by methyl pyronin-green staining, which showed diffuse staining of plasma cells, and B220/CD45R immunostaining, which highlighted the admixed small lymphocytes. Plasma cell infiltrates have been described as part of a reparative pro-

cess after various forms of lung injury.[30–32] Microarray analyses revealed immunoglobulin fragments in PKC$\delta^{-/-}$ mice lungs, a likely contribution of autoreactive antibodies in these mice that die prematurely because of autoimmune disease.[15,33] These results and methyl pyronin-green staining for plasma cells are consistent with the observation that plasma cells also accumulate in the lungs of PKC$\delta^{-/-}$ mice regardless of asbestos exposure. Although lymphoplasmacytic infiltration can be seen in pulmonary fibrosis induced by Fas antigen[34] and in interstitial lung disease in patients with systemic sclerosis,[35] sham PKC$\delta^{-/-}$ mice with plasma cell infiltrates did not develop fibrosis in our studies.

We observed early (3 day) alterations in a number of chemokines and cytokines in BALF that have been implicated in fibrosis.[2] Recent work from our laboratory demonstrated elevations in BALF of several profibrotic Th2 cytokines, ie, IL-4 and IL-6, at 9 days after initiation of asbestos inhalation.[14] Moreover, we report here significant elevations in IL-13, a major effector molecule at sites of Th2 inflammation and lung remodeling,[36] in asbestos-exposed WT mice at 3 days. At this early time point, several cytokines (MIP-1α, MIP-1β, and RANTES)[37] and MCP-1 were also increased in BALF from these mice. These cytokines have been implicated as key contributors to bleomycin- and asbestos-induced fibrosis.[38,39] It is to be noted here that MCP-1, MIP-1α, and MIP-1β attract and activate NK cells and that both the chemokines and the responder target cells are decreased in asbestos-exposed PKC$\delta^{-/-}$ mice. In addition, levels of IL-5, IL-12 (p40), and IL-10 were elevated in asbestos-exposed WT mice. IL-5 plays a central role in the growth and differentiation of eosinophils and contributes to several disease states, including asthma. The regulation of IL-5 message is primarily at the level of transcription and is likely to be controlled, to a large extent, by regulatory elements in the promoter region that can influence the transcriptional activity of the gene.[40] IL-12 can activate cytotoxic lymphocytes, stimulate NK cell activity, induce production of IFN-γ, and inhibit the development of various experimental tumors. Recently it was shown that IL-12 induces IL-10 production by human T cells and NK cells, as a negative feedback for IL-12-induced immune response.[41] One study suggests a negative role for PKC-δ and positive role for PKC-ε in the regulation of LPS-stimulated IL-12p40 secretion from murine macrophages.[42] IL-10 is an immunosuppressive cytokine, and PKC-β(II) and δ isozymes are essential for the activation of this cytokine production in human monocytes after stimulation by HIV-1 Tat protein.[43]

The Bioplex data in Figure 2 reveal that protein levels of most cytokines were increased dramatically and significantly in asbestos-exposed WT mice in contrast to PKC$\delta^{-/-}$ mice at 3 days. However, at 9 days, levels of most cytokines in BALF were lower in asbestos-exposed WT mice and comparable with [IL-6, MIP-1α, KC, 1L-1β, G-CSF, IL-1α, IL-10, IL-12 (p70), RANTES], or significantly decreased (IL-13, MCP-1, IL-5, GM-CSF) from amounts seen in asbestos-inhaling PKC$\delta^{-/-}$ mice. This may reflect the possibility that asbestos fibers stimulating cytokine elaboration are translocated from sites of initial deposition in the airways to the peripheral lung throughout time. On the other hand, populations and properties of cytokine-producing cell types recruited to lung and BALF between 3 and 9 days may vary dramatically.

Inhalation of asbestos was also associated with elevated levels in BALF of the NF-κB-dependent proinflammatory proteins, GM-CSF and RANTES, which are synthesized by airway epithelial cells and other cell types. Similar to patterns described above for other cytokines, asbestos-associated GM-CSF and RANTES levels were highest in BALF from WT mice at 3 days but comparable with levels in asbestos-exposed PKC$\delta^{-/-}$ mice at 9 days. These observations suggest a key role of PKC-δ in the regulation of asbestos-induced NF-κB-dependent gene expression as has been indicated previously in airway epithelial cells.[44] Although links between PKC-δ and synthesis of IL-1β and IL-6 also have been reported in human monocytes *in vitro*,[12] our data are the first to link PKC-δ deficiency to altered cytokine expression in an animal model. Whether PKC-δ is critical to transcription, translation, and/or posttranslational modification of specific cytokines altered in asbestos-exposed PKC$\delta^{-/-}$ mice requires detailed studies with various lung cell types *in vitro*.

We observed many effects of PKC-δ deficiency here including inhibition of asbestos-associated peribronchiolar cell proliferation, alteration of immune cell profiles in lung and BALF, and modulation of cytokine profiles in BALF. Accordingly, it is difficult to determine whether the inhibition of asbestosis observed in PKC$\delta^{-/-}$ mice reflects indirect or direct effects of PKC-δ on lung matrix. For example, PKC-δ is critical in regulation of collagen gene expression,[8,9] and it has been suggested that

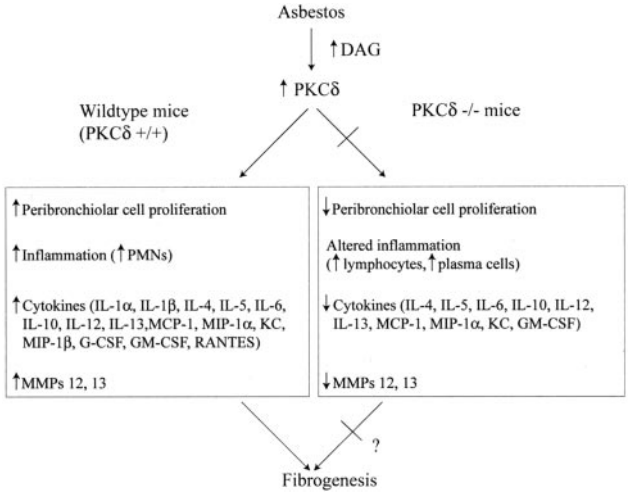

Figure 9. Mechanistic framework for increased PKC-δ activity by asbestos in normal (WT) lung and events occurring during the pathogenesis of fibrogenesis. Asbestos causes increased formation of diacylglycerol (DAG), an activator of PKCs[45] and increased expression of PKC-δ in lung tissue.[6] This then leads to increased peribronchiolar proliferation of $CD45^+$ leukocytes as well as $CD45^-$ fibroblasts, resulting in fibrosis. In addition, inflammation, the elaboration of several inflammatory and fibrogenic cytokines, and increased expression of MMP-12 and MMP-13[11] are seen. With knockout of PKC-δ, inhibition of asbestos-associated peribronchiolar cell proliferation occurs. In addition, altered inflammation and inhibition of inflammatory, neutrophil chemoattractant, and fibrogenic cytokines are observed as well as decreases in MMP-12 and MMP-13.[11]

transforming growth factor-β requires active PKC-δ to activate the target genes, collagen 1α1 and collagen 3α1, in a variety of cells *in vitro* including pulmonary fibroblasts.[9] Signaling by PKC-δ is also directly involved in the synthesis of fibronectin[10] and MMPs.[11] Using *in vitro* approaches and PKC$\delta^{-/-}$ mice, we have recently shown that transcriptional up-regulation of MMP-12 and MMP-13 by asbestos occurs via a PKC-δ-dependent pathway. Moreover, decreased levels of MMP-12 and MMP-13 mRNA were observed in the lungs of asbestos-exposed PKC$\delta^{-/-}$ mice.

Figure 9 presents a schema of events occurring in lung and BALF of asbestos-exposed WT mice that are altered in PKC$\delta^{-/-}$ mice. These novel findings and other mechanistic research from our laboratory support the hypothesis that modulation of early peribronchiolar cell proliferation, cytokine production, and immune cell profiles in BALF, lung, and spleen may alter the pathogenesis of asbestosis in PKC-δ deficiency. Whether these multiple systemic perturbations or direct effects of PKC-δ deficiency on lung matrices are critical to the modulation of fibrosis is difficult to determine and will require more protracted inhalation times with more fibrogenic types of amphibole asbestos. In addition, because PKC$\delta^{-/-}$ mice develop autoimmune disease,[15] we cannot exclude an effect of autoimmune disease on possible inhibition of asbestosis. Regardless, the therapeutic administration of PKC-δ inhibitors might be effective in prevention of fibroproliferative and other asbestos-associated lung and pleural diseases.

Acknowledgments

We thank Dr. David Hemenway and Justin Robbins, Votey Inhalation Facility, University of Vermont, for performing inhalation experiments; Colette Charland for running flow cytometer; and the Microscopy Imaging Facility at the University of Vermont and Maximilian MacPherson for performing Ki-67 staining.

References

1. Mossman BT, Bignon J, Corn M, Seaton A, Gee JB: Asbestos: scientific developments and implications for public policy. Science 1990, 247:294–301
2. Mossman BT, Churg A: Mechanisms in the pathogenesis of asbestosis and silicosis. Am J Respir Crit Care Med 1998, 157:1666–1680
3. Buchner K: The role of protein kinase C in the regulation of cell growth and in signalling to the cell nucleus. J Cancer Res Clin Oncol 2000, 126:1–11
4. Mellor H, Parker PJ: The extended protein kinase C superfamily. Biochem J 1998, 332:281–292
5. Tan SL, Parker PJ: Emerging and diverse roles of protein kinase C in immune cell signalling. Biochem J 2003, 376:545–552
6. Lounsbury KM, Stern M, Taatjes D, Jaken S, Mossman BT: Increased localization and substrate activation of protein kinase C delta in lung epithelial cells following exposure to asbestos. Am J Pathol 2002, 160:1991–2000
7. Shukla A, Stern M, Lounsbury KM, Flanders T, Mossman BT: Asbestos-induced apoptosis is protein kinase C delta-dependent. Am J Respir Cell Mol Biol 2003, 29:198–205
8. Zhang L, Keane MP, Zhu LX, Sharma S, Rozengurt E, Strieter RM, Dubinett SM, Huang M: Interleukin-7 and transforming growth factor-beta play counter-regulatory roles in protein kinase C-delta-dependent control of fibroblast collagen synthesis in pulmonary fibrosis. J Biol Chem 2004, 279:28315–28319
9. Jimenez SA, Gaidarova S, Saitta B, Sandorfi N, Herrich DJ, Rosenbloom JC, Kucich U, Abrams WR, Rosenbloom J: Role of protein kinase C-delta in the regulation of collagen gene expression in scleroderma fibroblasts. J Clin Invest 2001, 108:1395–1403
10. Mimura Y, Ihn H, Jinnin M, Asano Y, Yamane K, Tamaki K: Epidermal growth factor induces fibronectin expression in human dermal fibroblasts via protein kinase C delta signaling pathway. J Invest Dermatol 2004, 122:1390–1398
11. Shukla A, Barrett TF, Nakayama KI, Nakayama K, Mossman BT, Lounsbury KM: Transcriptional up-regulation of MMP12 and MMP13 by asbestos occurs via a PKCdelta-dependent pathway in murine lung. FASEB J 2006, 20:997–999
12. Kontny E, Ziolkowska M, Ryzewska A, Maslinski W: Protein kinase c-dependent pathway is critical for the production of pro-inflammatory cytokines (TNF-alpha, IL-1beta, IL-6). Cytokine 1999, 11:839–848
13. Robledo RF, Buder-Hoffmann SA, Cummins AB, Walsh ES, Taatjes DJ, Mossman BT: Increased phosphorylated extracellular signal-regulated kinase immunoreactivity associated with proliferative and morphologic lung alterations after chrysotile asbestos inhalation in mice. Am J Pathol 2000, 156:1307–1316
14. Sabo-Attwood T, Ramos-Nino M, Bond J, Butnor KJ, Heintz N, Gruber AD, Steele C, Taatjes DJ, Vacek P, Mossman BT: Gene expression profiles reveal increased mClca3 (Gob5) expression and mucin production in a murine model of asbestos-induced fibrogenesis. Am J Pathol 2005, 167:1243–1256
15. Miyamoto A, Nakayama K, Imaki H, Hirose S, Jiang Y, Abe M, Tsukiyama T, Nagahama H, Ohno S, Hatakeyama S, Nakayama KI: Increased proliferation of B cells and auto-immunity in mice lacking protein kinase Cdelta. Nature 2002, 416:865–869
16. Wylie AG, Skinner HC, Marsh J, Snyder H, Garzione C, Hodkinson D, Winters R, Mossman BT: Mineralogical features associated with cytotoxic and proliferative effects of fibrous talc and asbestos on rodent tracheal epithelial and pleural mesothelial cells. Toxicol Appl Pharmacol 1997, 147:143–150
17. Peng SL, Gerth AJ, Ranger AM, Glimcher LH: NFATc1 and NFATc2 together control both T and B cell activation and differentiation. Immunity 2001, 14:13–20
18. Craighead JE, Abraham JL, Churg A, Green FH, Kleinerman J, Pratt PC, Seemayer TA, Vallyathan V, Weill H: The pathology of asbestos-associated diseases of the lungs and pleural cavities: diagnostic criteria and proposed grading schema. Report of the Pneumoconiosis Committee of the College of American Pathologists and the National Institute for Occupational Safety and Health. Arch Pathol Lab Med 1982, 106:544–596
19. Evans CM, Williams OW, Tuvim MJ, Nigam R, Mixides GP, Blackburn MR, DeMayo FJ, Burns AR, Smith C, Reynolds SD, Stripp BR, Dickey BF: Mucin is produced by Clara cells in the proximal airways of antigen-challenged mice. Am J Respir Cell Mol Biol 2004, 31:382–394
20. Haegens A, van der Vliet A, Butnor KJ, Heintz N, Taatjes D, Hemenway D, Vacek P, Freeman BA, Hazen SL, Brennan ML, Mossman BT: Asbestos-induced lung inflammation and epithelial cell proliferation are altered in myeloperoxidase-null mice. Cancer Res 2005, 65:9670–9677
21. Davis GS, Pfeiffer LM, Hemenway DR: Interferon-gamma production by specific lung lymphocyte phenotypes in silicosis in mice. Am J Respir Cell Mol Biol 2000, 22:491–501
22. Shukla A, Timblin C, BeruBe K, Gordon T, McKinney W, Driscoll K, Vacek P, Mossman BT: Inhaled particulate matter causes expression of nuclear factor (NF)-kappaB-related genes and oxidant-dependent NF-kappaB activation in vitro. Am J Respir Cell Mol Biol 2000, 23:182–187
23. Crystal RG, Bitterman PB, Mossman B, Schwarz MI, Sheppard D, Almasy L, Chapman HA, Friedman SL, King Jr TE, Leinwand LA, Liotta L, Martin GR, Schwartz DA, Schultz GS, Wagner CR, Musson RA: Future research directions in idiopathic pulmonary fibrosis: summary of a National Heart, Lung, and Blood Institute working group. Am J Respir Crit Care Med 2002, 166:236–246
24. BéruBé KA, Quinlan TR, Moulton G, Hemenway D, O'Shaughnessy P, Vacek P, Mossman BT: Comparative proliferative and histopathologic

changes in rat lungs after inhalation of chrysotile or crocidolite asbestos. Toxicol Appl Pharmacol 1996, 137:67–74
25. Jackson DN, Foster DA: The enigmatic protein kinase Cdelta: complex roles in cell proliferation and survival. FASEB J 2004, 18:627–636
26. Chou WH, Choi DS, Zhang H, Mu D, McMahon T, Kharazia VN, Lowell CA, Ferriero DM, Messing RO: Neutrophil protein kinase Cdelta as a mediator of stroke-reperfusion injury. J Clin Invest 2004, 114:49–56
27. Armstrong DA, Major JA, Chudyk A, Hamilton TA: Neutrophil chemoattractant genes KC and MIP-2 are expressed in different cell populations at sites of surgical injury. J Leukoc Biol 2004, 75:641–648
28. Kamp DW, Dunn MM, Sbalchiero JS, Knap AM, Weitzman SA: Contrasting effects of alveolar macrophages and neutrophils on asbestos-induced pulmonary epithelial cell injury. Am J Physiol 1994, 266:L84–L91
29. Kim JH, Kim HY, Kim S, Chung JH, Park WS, Chung DH: Natural killer T (NKT) cells attenuate bleomycin-induced pulmonary fibrosis by producing interferon-gamma. Am J Pathol 2005, 167:1231–1241
30. Gonzalez-Moya JE, Hueto J, Ruiz de Azua AY, Sanchez J, Franquet T: Evolution of a case of lung plasma cell granuloma. Eur Respir J 1991, 4:755–757
31. Spencer H: The pulmonary plasma cell/histiocytoma complex. Histopathology 1984, 8:903–916
32. Balachandran A, Shivbalan S: Plasma cell granuloma of the lung. Indian Pediatr 2004, 41:292–293
33. Mecklenbräuker I, Saijo K, Zheng NY, Leitges M, Tarakhovsky A: Protein kinase Cdelta controls self-antigen-induced B-cell tolerance. Nature 2002, 416:860–865
34. Hagimoto N, Kuwano K, Nomoto Y, Kunitake R, Hara N: Apoptosis and expression of Fas/Fas ligand mRNA in bleomycin-induced pulmonary fibrosis in mice. Am J Respir Cell Mol Biol 1997, 16:91–101
35. Harrison NK, Myers AR, Corrin B, Soosay G, Dewar A, Black CM, Du Bois RM, Turner-Warwick M: Structural features of interstitial lung disease in systemic sclerosis. Am Rev Respir Dis 1991, 144:706–713
36. Elias JA, Lee CG, Zheng T, Shim Y, Zhu Z: Interleukin-13 and leukotrienes: an intersection of pathogenetic schema. Am J Respir Cell Mol Biol 2003, 28:401–404
37. Lee PJ, Zhang X, Shan P, Ma B, Lee CG, Homer RJ, Zhu Z, Rincon M, Mossman BT, Elias JA: ERK1/2 mitogen-activated protein kinase selectively mediates IL-13-induced lung inflammation and remodeling in vivo. J Clin Invest 2006, 116:163–173
38. Smith RE, Strieter RM, Phan SH, Kunkel SL: C-C chemokines: novel mediators of the profibrotic inflammatory response to bleomycin challenge. Am J Respir Cell Mol Biol 1996, 15:693–702
39. Driscoll KE, Hassenbein DG, Carter J, Poynter J, Asquith TN, Grant RA, Whitten J, Purdon MP, Takigiku R: Macrophage inflammatory proteins 1 and 2: expression by rat alveolar macrophages, fibroblasts, and epithelial cells and in rat lung after mineral dust exposure. Am J Respir Cell Mol Biol 1993, 8:311–318
40. Liu C, Lu J, Tan J, Li L, Huang B: Human interleukin-5 expression is synergistically regulated by histone acetyltransferase CBP/p300 and transcription factors C/EBP, NF-AT and AP-1. Cytokine 2004, 27:93–100
41. Takeuchi E, Yanagawa H, Suzuki Y, Shinkawa K, Ohmoto Y, Bando H, Sone S: IL-12-induced production of IL-10 and interferon-gamma by mononuclear cells in lung cancer-associated malignant pleural effusions. Lung Cancer 2002, 35:171–177
42. Fronhofer V, Lennartz MR, Loegering DJ: Role of PKC isoforms in the Fc(gamma)R-mediated inhibition of LPS-stimulated IL-12 secretion by macrophages. J Leukoc Biol 2006, 79:408–415
43. Contreras X, Bennasser Y, Bahraoui E: IL-10 production induced by HIV-1 Tat stimulation of human monocytes is dependent on the activation of PKC beta(II) and delta isozymes. Microbes Infect 2004, 6:1182–1190
44. Page K, Li J, Zhou L, Iasvovskaia S, Corbit KC, Soh JW, Weinstein IB, Brasier AR, Lin A, Hershenson MB: Regulation of airway epithelial cell NF-kappa B-dependent gene expression by protein kinase C delta. J Immunol 2003, 170:5681–5689
45. Sesko A, Cabot M, Mossman B: Hydrolysis of inositol phospholipids precedes cellular proliferation in asbestos-stimulated tracheobronchial epithelial cells. Proc Natl Acad Sci USA 1990, 87:7385–7389